Ultrafast time-resolved spectroscopy of one-dimensional metal-dielectric photonic crystals

T. Ergin, T. Benkert, H. Giessen, and M. Lippitz*
4. Physikalisches Institut, Universität Stuttgart, Pfaffenwaldring 57, 70550 Stuttgart, Germany
and Max-Planck-Institut für Festkörperforschung, Heisenbergstr. 1, 70569 Stuttgart, Germany
(Received 10 March 2009; revised manuscript received 28 May 2009; published 29 June 2009)

We study the all-optical switching behavior of one-dimensional metal-dielectric photonic crystals due to the nonlinearity induced by a hot electron gas. A polychromatic pump-probe setup is used to determine the wavelength and pump intensity dependence of the ultrafast transmission suppression as well as the dynamics of the process on a subpicosecond time scale. We find ultrafast (subpicosecond) as well as a slow (millisecond) behavior. We present a model of the ultrafast dynamics and nonlinear response, which can fit the measured data well and allows us to separate the thermal and the electronic response of the system.

DOI: 10.1103/PhysRevB.79.245134 PACS number(s): 42.70.Qs, 42.65.−k

I. INTRODUCTION

In the late 1980s, the field of photonic crystals emerged.[1–3] Since then it has rapidly evolved and grown more interesting to a wide community. Photonic crystals show remarkable properties due to their band structure, which lead to the realization of a number of applications, such as bending of light around 120° corners,[4] extremely slow light in a medium,[5] and negative refraction while keeping the index of refraction positive.[6]

Another promising field of application is the combination of photonic and electronic devices or even the replacement of electronics by photonics or plasmonics.[7] Such all-optical circuits have several advantages over conventional electronics, such as reduced size, high repetition rates, and enhanced speed of operation.[9]

A key component for such circuits is an all-optical switch. One-dimensional metal-dielectric photonic crystals (1DMDPCs) might fulfill this purpose as small pump-induced variations in the dielectric properties can lead to strong transmission changes. In this paper we study experimentally the suitability of 1DMDPCs for ultrafast switching in the subpicosecond regime, determine the detailed wavelength and intensity dependences, and give a theoretical model, which agrees well with our experimental data.

A 1DMDPC is a structure that exhibits a periodic change in the index of refraction in one dimension. Alternating layers of metal and dielectric are deposited with a subwavelength thickness. This gives rise to a photonic band structure with passbands and stop bands in the transmission spectrum. A large amount of metal can thus be accumulated in these structures while keeping them transparent.[8] This unique feature allows us to exploit the nonlinear properties of the constituting materials.[9] Various properties and possible applications have been proposed based on numerical calculations and experiments, for example, optical limiting, switching, and selective shielding.[8,10–12] However, the time constant of the nonlinear response of such structures was not measured. While previous work made use of the strong nonlinearity of the bound metal electrons, we explore the possibility of using the response of the free electrons. That approach has the advantage that no material resonance is involved and thus the whole device could be tailored over a much larger spectral range.

II. EXPERIMENTAL TECHNIQUES

We use a polychromatic pump-probe setup to investigate the 1DMDPC. The laser system consists of a Ti:Sa oscillator, which is pumped with 10 W at 532 nm. This gives rise to 1.5 W average power and a pulse length of 200 fs at 825 nm. The repetition rate of the mode-locked laser system is 76 MHz. We split the beam into a pump and a probe arm. The pump-arm length is tunable mechanically, which allows high temporal resolution of our setup, limited only by the pulse length. We modulate the pump beam with an acousto-optical modulator (AOM) at 100 kHz for lock-in detection. In a second beam path, a tapered fiber[13] is used to generate a white light continuum from which the probe pulse is shaped in the time as well as in the frequency domain. This allows us to choose the probe pulse central wavelength and width while still keeping the pulse duration at 600 fs. The pulses are overlapped in a polarizing beam-splitter cube and focused collinearly on the sample. Behind the sample the pump beam is filtered out spectrally and a balanced receiver detects the transmitted probe power.

The samples are prepared using an electron-beam evaporation technique. Alternating layers of Ag and MgF_2 are evaporated on a quartz substrate at a pressure of 10^{-7} mbar. The metal is evaporated with a rate of 20 Å/s to avoid clustering and to achieve smooth films since otherwise silver tends to cluster when applied at such small thicknesses.[14,15] The smoothness of the film, on the other hand, is critical for consistent measurements. For reasons that become obvious below, we name each sample by the number of cavities formed between consecutive metal layers. Two samples were used in this work: a single cavity sample (substrate-Ag-MgF_2-Ag-MgF_2 with 30 nm Ag and 225 nm MgF_2) and a double cavity sample (substrate-Ag-MgF_2-Ag-MgF_2-Ag-MgF_2 with 20 nm Ag and 215 nm MgF_2). The first has a narrow transmission resonance at 720 nm and the latter at 705 and 810 nm.

III. LINEAR TRANSMISSION PROPERTIES

In a first step, it is instructive to look at the linear transmission spectra of 1DMDPCs and their band structure. Figure 1 shows a measured transmission spectrum of the double

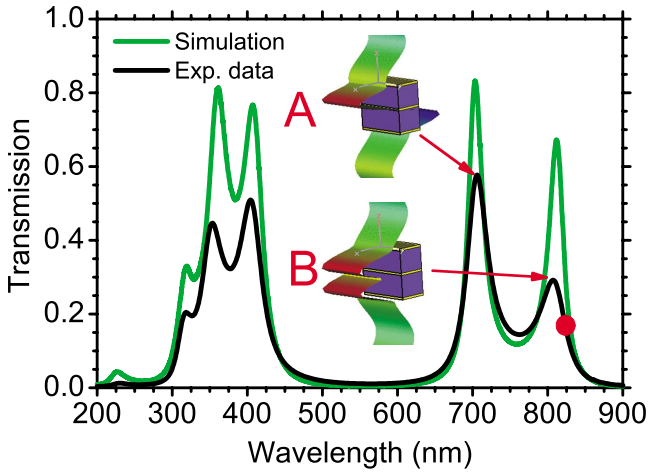

FIG. 1. (Color online) Measured linear transmission spectrum of the "double cavity" 1DMDPC. Passbands with multiple transmission peaks occur. The simulated spectrum was calculated using the transfer-matrix method. The dot indicates the fixed pump wavelength used in this paper. The insets show electric field distributions at the wavelengths marked with the arrow superimposed on the structure (thin layer: Ag; thick layer: MgF_2). The field forms standing waves with a symmetric (**B**) and antisymmetric (**A**) mode and nodes only at the metal layers. The transmission peaks at smaller wavelengths correspond to higher order modes with an additional node in the center of each MgF_2 layer.

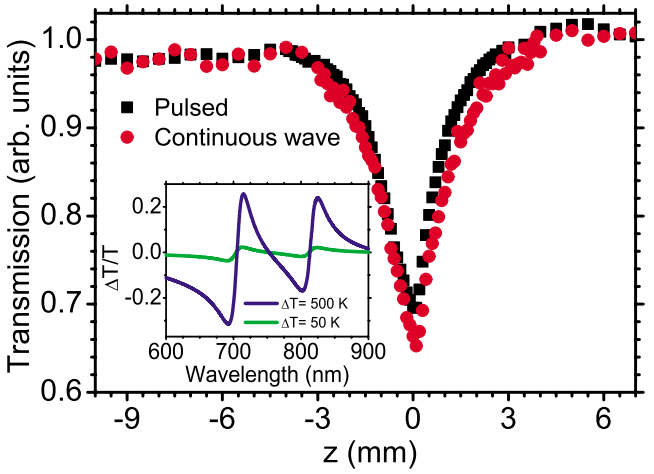

FIG. 2. (Color online) Open aperture z-scan measurement of the double cavity sample at a pump wavelength of 825 nm (see dot in Fig. 1). The sample was measured with a continuous wave and a pulsed laser beam with the same average power (20 mW) but peak powers differing by about five orders of magnitude. The inset shows the calculated differential transmission due to thermal effects. The assumed temperature modulation is $\Delta T = 50$ and 500 K starting from room temperature.

cavity sample. Calculations using the transfer-matrix method[16,17] reproduce the features very well. Each passband (around 700–850 and around 300–450 nm) is approximately 150 nm wide and consists of two peaks. The small third peak in the passband at 310 nm is due to the interband transition of silver. To understand these features, we consider the Bragg condition.[18,19] The metal layers form Bragg planes, which are separated by dielectric layers of thickness d. This leads to standing waves inside the structure if the condition $nd = k\lambda_0/2$ is fulfilled, where n is the refractive index, λ_0 is the wavelength in vacuum, and k is an integer. However, the Bragg model is only a first approximation, as according to it the long-wavelength passband should occur at 675 nm and have only one peak.

We can also regard our system as coupled cavities. Each layer series of metal-dielectric-metal forms a cavity. Consecutive cavities are coupled by the electric field leaking through the joining metal layer. A series of N cavities can be described by a series of N coupled oscillators that exhibit N eigenmodes. The inset of Fig. 1 shows the electric field distribution for the symmetric and antisymmetric eigenmodes of the lowest-order passband, calculated with a finite-difference time-domain (FDTD) method. The second-order modes (around 300–450 nm) have an additional node of the field in the center of each cavity (not shown).

The separation between two eigenfrequencies, i.e., two transmission peaks, is given through the coupling strength of the oscillators, i.e., the thickness of the silver layer. A thinner metal layer corresponds to a stronger coupling of the cavity system since the evanescent light field decays exponentially inside the silver. The transmission is lower for the symmetric fundamental mode (marked B), as the electric field undergoes a π phase jump at the silver layer, which leads to a higher field inside the metal and therefore to a greater loss.

IV. THERMAL EFFECTS

In contrast to experiments at a low laser repetition rate,[9] our repetition rate of 76 MHz leads to a larger power absorbed in the sample at even moderate pulse energies. The temperature rise can reach several hundreds of kelvins locally and thermal effects have to be considered. Any change in the optical properties due to temperature will lead to a cavity detuning and thus to a change in transmission that could mislead the interpretation of experiments that do not contain temporal information on the picosecond time scale, such as z-scan experiments.[9,20] A z-scan[21] is a single beam experiment, where the sample is moved through the focus along the optical axis (z axis) of the beam. The transmission is measured depending on the z position of the sample, i.e., as a function of the laser intensity, as the focus size varies. Such measurements are used to determine the nonlinear absorption coefficient and the nonlinear refractive index. Our laser system allows us to switch between mode locked and continuous-wave mode, changing thus the peak power by about five orders of magnitude without changing the average impinging power. Figure 2 depicts the results of an open aperture z-scan measurement of the double cavity sample at a pump wavelength of 825 nm and a focal length of 50 mm. In our case, the change in transmission during the z-scan is not due to effects that are nonlinear in the instantaneous optical field strength, as the field strength differs by a factor of about 300 between the two curves. The transmission change is only related to the deposited energy in the system and thus the heat load. The long time constant of the thermal effect averages over the laser pulses. A measurement of the time con-

stants while the sample is in the laser focus yields for the rise and decay times values of 230 and 1570 ms, respectively.

A thermal response of the 1DMDPC can have several sources: thermal expansion due to the thermal expansion coefficient δ, change in the index of refraction due to the thermo-optic coefficient Γ, change in the index of refraction due to the nonlinear refractive index n_2, and change in the plasma frequency of the metal in an expanded layer. The last two points are negligible since the layer expansion and thermo-optic effects are orders of magnitude larger for the materials used in our experiment. The inset of Fig. 2 shows the calculated differential transmission for temperature variations ΔT of 50 and 500 K starting from room temperature using the transfer-matrix method. The parameters[22] for this calculation are $\delta_{Ag}=1.89\times10^{-5}$ K^{-1}, $\delta_{MgF_2}=1\times10^{-5}$ K^{-1}, and $\Gamma_{MgF_2}=2\times10^{-6}$ K^{-1}. The calculated effect reaches the same order as the measured transmission change in the z scan.

V. TIME-RESOLVED ULTRAFAST EXPERIMENTS

To avoid the ambiguity of z-scan measurements with respect to thermal effects, we now turn to time-resolved pump-probe experiments on the picosecond time scale. They will allow us not only to separate the influence of heat accumulation on a millisecond time scale from ultrafast effects but also to gain the time constants of the ultrafast response of the 1DMDPC.

A. Ultrafast response of metals

The ultrafast response of the 1DMDPC is governed by the response of the metal layers, which can be separated into four phases that overlap in time:[23–25]

(1) Pump photons excite some free electrons into higher levels far above the Fermi level, which leads to a non-Fermi-Dirac distribution since most of the electrons are still "cold." Our pulses of 600 fs length cannot resolve this short phase.[26]

(2) In a few tens to hundreds of femtoseconds, the electron gas thermalizes via electron-electron scattering to a Fermi-Dirac distribution. Electron-gas temperatures of several hundreds to a few thousand kelvins can be reached. As our experiment in the near infrared probes the free electrons, this phase leads to the highest system response.

(3) The electron gas transfers its energy to the lattice via electron-phonon coupling. Due to the large heat capacity of the lattice, a single laser pulse increases the temperature by only a few ten kelvins.

(4) The coupled system cools down to the same temperature as outside the laser spot. The accumulated absorbed energy together with the slow heat conduction away from the laser spot leads to the temperature increase of some hundreds of kelvins, as discussed in Sec. IV.

As soon as a thermal distribution of the excited electrons is reached, the coupled electron-lattice system can be described by the two-temperature model (TTM).[27] The temperatures of the electron gas and the lattice (T_e and T_l) are given by two coupled differential equations,

$$C_e\frac{\partial T_e}{\partial t} = -g(T_e - T_l) + \vec{\nabla}\kappa\vec{\nabla}T_e + S, \tag{1}$$

$$C_l\frac{\partial T_l}{\partial t} = g(T_e - T_l), \tag{2}$$

where $C_e=\alpha T_e$ is the specific heat capacity of the electron gas, κ is the heat diffusion coefficient, S is the source term, g describes the electron-phonon coupling, and C_l is the specific heat capacity of the lattice. The temperatures and the source term are functions of space and time. To simplify the calculations, we avoid a full spatial treatment of the system by neglecting the spatial dependence and by replacing the exact heat diffusion term with an empiric diffusion term including a fit parameter d, which couples the system to a temperature bath at room temperature T_{room}. This accounts for the heat transport out of the system, which is hereby assumed to be governed by the electron gas. The equations are then reduced to

$$\frac{\partial T_e}{\partial t} = -\frac{g(T_e - T_l)}{\alpha T_e} - d(T_e - T_{room}) + \frac{S}{\alpha T_e}, \tag{3}$$

$$\frac{\partial T_l}{\partial t} = \frac{g(T_e - T_l)}{C_l}. \tag{4}$$

The parameters[23] for the simulations are $\alpha=66$ J/(m^3 K^2), $g=3\times10^{16}$ W/(m^3 K), and $C_l=2.415\times10^6$ J/(m^3 K). We chose C_l to be constant since we measure at a temperature well above the Debye temperature of silver ($\approx$200 K). The source term is assumed to be a Gaussian pulse (in time) that is absorbed in a spot of 10 μm diameter. For reasons of simplicity, we assume the whole pulse energy to be absorbed in these numerical calculations.

For the calculation of the transient transmission suppression we incorporate the TTM into the transfer matrix and reference the work of Bigot *et al.*[23] The electron gas and lattice temperature are calculated using the TTM. To account for the change in the optical properties, the dielectric function $\epsilon(\omega)$ of the metal layer is modified, starting from Johnson and Christy[14] values, with a Drude term for the free electrons that depends on the rise of the electron-gas temperature ΔT_e,

$$\epsilon(\omega,\Delta T_e) = \epsilon_{J+C}(\omega) - \epsilon_{Drude}(\omega,\Delta T_e = 0) + \epsilon_{Drude}(\omega,\Delta T_e). \tag{5}$$

The Drude model is made temperature dependent by letting the damping constant γ depend on ΔT_e. This is motivated as with increasing electron-gas temperature the Fermi distribution smears out and more and more possibilities for electron-electron scattering occur. We set[23]

$$\gamma(\Delta T_e) = \gamma_0 + \beta\Delta T_e, \tag{6}$$

where β is a fit parameter in our calculations and γ_0 is the room temperature value of the damping constant. The modified Drude model reads thus

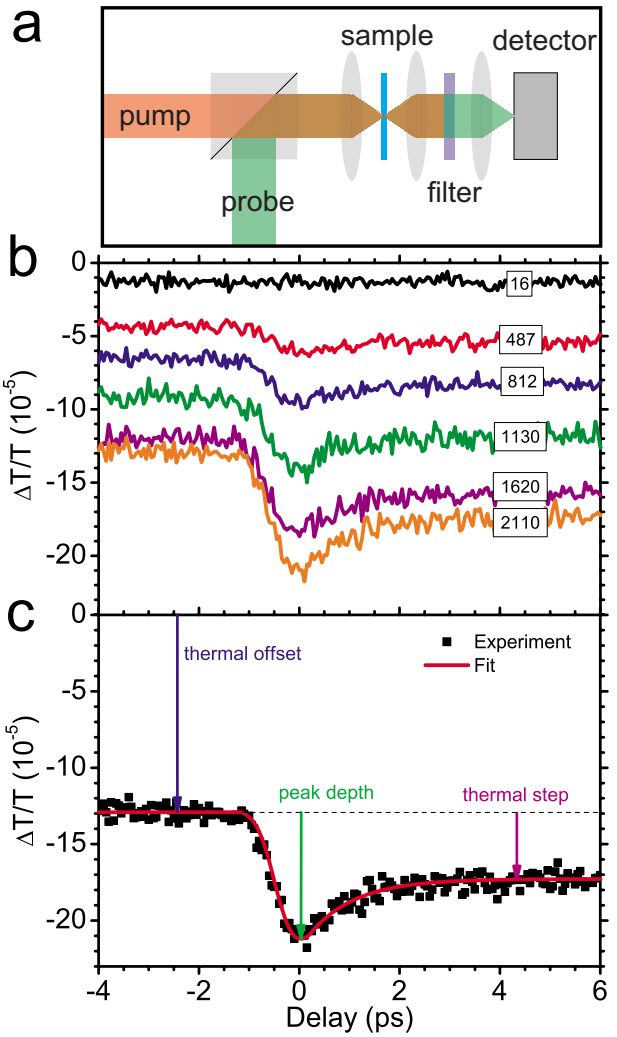

FIG. 3. (Color online) (a) Detection part of the experimental setup. (b) Pump-probe measurements with varying pump intensity (given in MW/cm^2 as numbers in the graph) on the single cavity sample. The absolute zero delay was set to the differential transmission peak minimum. The sample was pumped at 825 nm and probed at 720 nm. (c) Example of the model function [Eq. (8)] fitted to one data set from (b).

$$\epsilon_{\mathrm{Drude}}(\omega,\Delta T_e) = \epsilon_\infty - \frac{\omega_p^2}{\omega[\omega + i\gamma(\Delta T_e)]}, \tag{7}$$

where ω_p is the plasma frequency.

B. Temporal dynamics of the nonlinear optical response

Our pump-probe setup [Fig. 3(a)] allows us to investigate not only the amplitude but also the temporal dynamics of the nonlinear optical effects in 1DMDPCs. A pump pulse is absorbed, which modifies the dielectric properties of the metal layers, and a probe pulse interrogates the transmission of the photonic crystal after a variable delay. Figure 3(b) shows a series of such measurements on the single cavity sample with varying intensity. The differential transmission is not zero for negative delays (i.e., probe arrives before pump) because of the thermal effect discussed above. This offset decreases with increasing AOM modulation frequency as less heat is accumulated in each AOM cycle. The probe transmission drops at the arrival of the pump pulse and recovers on a subpicosecond time scale. It does not recover fully to the start value since also the last pump pulse deposits additional heat in the focal area.

To extract quantitative data from these traces and similar ones from the double cavity sample, we fitted a phenomenological model function $f(\tau)$ to the data,

$$f(\tau) = A + [Be^{-\tau/\tau_0} + C(1 - e^{-\tau/\tau_0})]\Theta(\tau). \tag{8}$$

A describes the amplitude of the thermal offset at negative delays. B is the amplitude of the response caused by the hot electron gas that decays exponentially with a time constant τ_0. The thermal effect of the pump pulse is taken into account by a level C that is exponentially approached with the same time constant τ_0. The last two processes start as soon as the pump pulse arrives, i.e., the Heaviside step function $\Theta(\tau)$ switches from 0 ($\tau<0$) to 1 ($\tau>0$). To take into account the limited temporal resolution of our setup, we convolute the model function $f(\tau)$ with a measured cross-correlation function between pump and probe pulse before fitting it to the data. A fit to a temporal trace at high pump power is shown in Fig. 3(c).

C. Intensity dependence of the nonlinear optical response

The amplitude B and the decay time τ_0 of the nonlinear optical response were recovered by fitting the phenomenological model function $f(\tau)$ to a set of temporal traces with different pump intensities. Figure 4 shows the data for the single and the double cavity samples. The absolute value of the nonlinear optical response $|B|$ seems to grow linear with pump intensity for both samples, always maintaining its negative sign. The decay time τ_0 is not constant but also increases with pump intensity. Both effects can be described by a TTM that modifies the Drude damping in the metal's dielectric properties as described in Sec. V A. Only two fit parameters are used for both parts of Fig. 4: first the relation between the increase in electron-gas temperature ΔT_e and Drude damping γ, described by β in Eq. (6), and second the empirical constant d to describe the heat diffusion by electrons in Eq. (3). The fit leads to $\beta = 6\times10^{-8}$ eV/K and $d = 3.7\times10^{11}$ s^{-1}. The deviations at small pump intensities for the single cavity sample in Fig. 4(b) might occur due to a lesser sample quality and to slightly different probe locations on the sample, which lead to locally changed heat diffusion and therefore to changed dynamics.

The temporal response in the 1DMDPCs is on the order of 1 ps. The effect of rising time constants with increasing pump intensity can be understood since the heat capacity of the electron gas is proportional to its temperature ($C_e = \alpha T_e$). The lattice heat capacity is orders of magnitude larger but higher pump intensities lead to a smaller difference between electron gas and lattice heat capacity. This leads to a slower equilibration (longer response time) and to a slightly higher end temperature. When the electron-gas heat capacity is assumed to be constant, for example, at its value at $T_e = 400$ K [$C_e = 2.64\times10^4$ J/(m^3 K)], then the time constant is

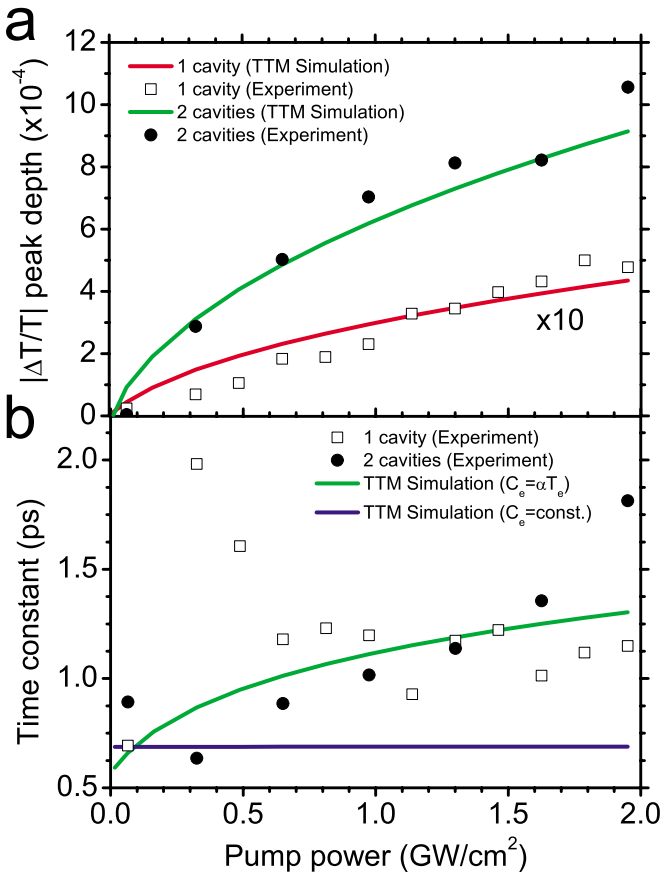

FIG. 4. (Color online) The TTM combined with a temperature-dependent Drude model describes with one parameter set pump-power dependence of both (a) the peak depth (amplitude B) as well as (b) the recovery time constant τ_0 of the ultrafast transmission suppression. The latter is weakly dependent on the pump intensity due to the temperature dependence of the electron heat capacity.

independent of the pump intensity [see horizontal line in Fig. 4(b)]. This confirms the temperature-dependent electron heat capacity as origin of the pump intensity dependence of the decay time. The general trend of increasing response times at higher pump intensities was also found in single layers of metal.[28] The values of the time constants were on the order of 1–2 ps.

To compare the magnitude of the nonlinear optical response of the 1DMDPCs with other materials, it is instructive to calculate the phenomenological nonlinear absorption coefficient α_{eff}. It describes the intensity dependence of the absorption coefficient α,

$$\alpha(I) = \alpha_0 + \alpha_{\text{eff}} I. \tag{9}$$

As the absorption coefficient α is connected to the transmission T via the sample thickness L: $T = T_0 e^{-\alpha L}$, the nonlinear absorption coefficient α_{eff} is just a measure for the slope of a linear fit to the data in Fig. 4(a). We obtain values of 5.2×10^{-10} and 7.4×10^{-9} cm/W for the single and double cavity samples, respectively, using as sample thickness L the sum of all metal and dielectric layers in the multilayer structure.

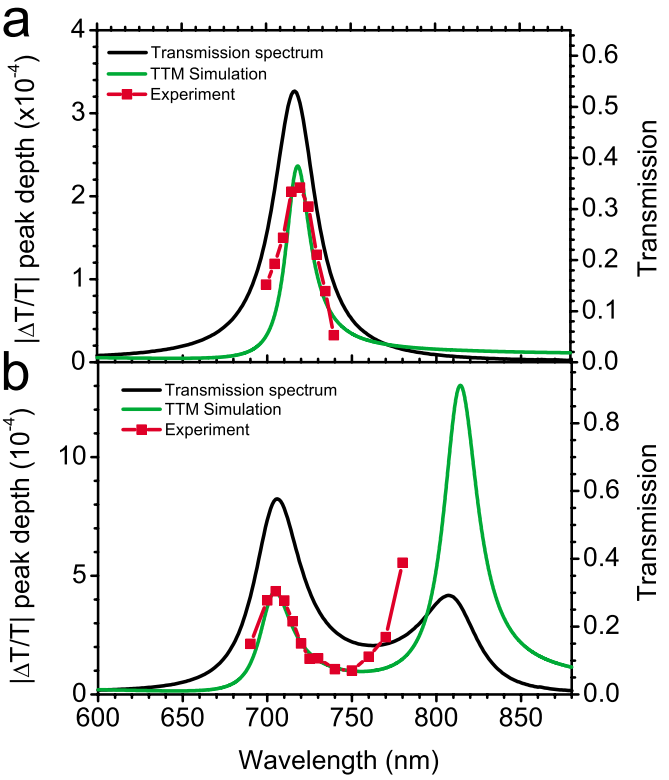

FIG. 5. (Color online) Spectral dependence of the transient transmission compared to the linear transmission spectrum and the model for (a) the single cavity sample and (b) the double cavity sample. The pump power (1.3 GW/cm^2) and pump wavelength (825 nm) were kept constant. The TTM simulations give a good agreement.

D. Wavelength dependence of the nonlinear optical response

Figure 5(a) shows the wavelength dependence of the ultrafast transmission suppression in the single cavity sample. For this measurement, pump power and pump wavelength were kept constant (1.3 GW/cm^2 at 825 nm). The shape of the differential transmission data follows the linear transmission spectrum, which means that the spectral response of an all-optical switch could be tuned by adjusting the thickness of the metal and dielectric layers.

The double cavity sample shows a similar behavior [Fig. 5(b)]. The TTM simulations predict a stronger response at the 810 nm transmission peak compared to the peak at 705 nm. The same trend is found in the experiment. However, the probe spectral range is limited by the pump filter stop band starting at 780 nm. The measurement shows a steeper rise than the simulations at 775 nm. This might be due to the roughness and inhomogeneity of the silver films. The position of the 810 nm peak is dependent on the silver layer thickness and the position of the 705 nm peak is relatively insensitive to thickness variations. The white light transmission spectrum is measured with a large spot (4 mm in diameter), which averages over the roughness. The pump-probe measurements, on the other hand, were performed with a spot size of roughly 10 μm. If a region with a slightly larger silver thickness was measured, the result would be a shift of the 810 nm peak into the blue, which would explain the rise

at smaller wavelengths. The TTM parameters for these simulations are $\beta=1.1\times10^{-8}$ eV/K and $\beta=3.5\times10^{-8}$ eV/K for the single and the double cavity samples, respectively.

VI. CONCLUSION

We have shown that one-dimensional metal-dielectric photonic crystals respond on two time scales to a near-infrared pump pulse train at a megahertz repetition rate: on a time scale of hundreds of milliseconds thermal effects lead to a large transmission change of 30–40 %. Simulations based on the transfer matrix were presented to explain the measurements. On a picosecond time scale, the ultrafast response of the metal's free electrons dominates. Its magnitudes are in the order of 10^{-5} in a single cavity system and 10^{-3} in a double cavity system. The two-temperature model and a temperature-dependent Drude model explain both the pump intensity and the probe wavelength dependence of the effect. Using the nonlinear response induced by a hot electron gas makes it possible to tune the spectral response of the metal-dielectric photonic crystal by its structure, i.e., without changing the material. However, that flexibility is accompanied by a reduced nonlinearity compared to material resonances.[12,20]

ACKNOWLEDGMENTS

We thank S. Linden (University of Karlsruhe) for the preparation of a sample. We acknowledge financial support by DFG (Grant Nos. FOR 557 and 730) and BMBF (Grant Nos. 13N9155 and 13N10146).

*m.lippitz@physik.uni-stuttgart.de

[1] E. Yablonovitch, Phys. Rev. Lett. **58**, 2059 (1987).
[2] S. John, Phys. Rev. Lett. **58**, 2486 (1987).
[3] J. D. Joannopoulos, R. D. Meade, and J. N. Winn, *Photonic Crystals: Molding the Flow of Light* (Princeton University, Princeton, 1995).
[4] M. Tokushima, H. Kosaka, A. Tomita, and H. Yamada, Appl. Phys. Lett. **76**, 952 (2000).
[5] H. Gersen, T. J. Karle, R. J. P. Engelen, W. Bogaerts, J. P. Korterik, N. F. van Hulst, T. F. Krauss, and L. Kuipers, Phys. Rev. Lett. **94**, 073903 (2005).
[6] E. Cubukcu, K. Aydin, E. Ozbay, S. Foteinopoulou, and C. M. Soukoulis, Nature (London) **423**, 604 (2003).
[7] K. F. MacDonald, Z. L. Samson, M. I. Stockman, and N. I. Zheludev, Nat. Photonics **3**, 55 (2009).
[8] M. Scalora, M. J. Bloemer, A. S. Pethel, J. P. Dowling, C. M. Bowden, and A. S. Manka, J. Appl. Phys. **83**, 2377 (1998).
[9] N. N. Lepeshkin, A. Schweinsberg, R. S. Bennink, and R. W. Boyd, Phys. Rev. Lett. **93**, 123902 (2004).
[10] M. Scalora, J. P. Dowling, C. M. Bowden, and M. J. Bloemer, Phys. Rev. Lett. **73**, 1368 (1994).
[11] M. J. Bloemer and M. Scalora, Appl. Phys. Lett. **72**, 1676 (1998).
[12] T. K. Lee, A. D. Bristow, J. Hubner, and H. M. van Driel, J. Opt. Soc. Am. B **23**, 2142 (2006).
[13] J. Teipel, K. Franke, D. Türke, F. Warken, D. Meiser, M. Leuschner, and H. Giessen, Appl. Phys. B: Lasers Opt. **77**, 245 (2003).
[14] P. B. Johnson and R. W. Christy, Phys. Rev. B **6**, 4370 (1972).
[15] L. Holland, *Vacuum Deposition of Thin Films* (Halsted, New York, 1956).
[16] F. L. Pedrotti, L. M. Pedrotti, and L. S. Pedrotti, *Introduction to Optics* (Cummings, Upper Saddle River, NJ, 2006).
[17] H. A. Macleod, *Thin-Film Optical Filters* (Taylor & Francis, London, 2001).
[18] A. Husakou and J. Herrmann, Phys. Rev. Lett. **99**, 127402 (2007).
[19] M. Hübner, J. P. Prineas, C. Ell, P. Brick, E. S. Lee, G. Khitrova, H. M. Gibbs, and S. W. Koch, Phys. Rev. Lett. **83**, 2841 (1999).
[20] Nir Rotenberg, A. D. Bristow, Markus Pfeiffer, Markus Betz, and H. M. van Driel, Phys. Rev. B **75**, 155426 (2007).
[21] M. Sheik-Bahae, A. A. Said, T.-H. Wei, D. J. Hagan, and E. W. V. Stryland, IEEE J. Quantum Electron. **26**, 760 (1990).
[22] M. J. Weber, *Handbook of Optical Materials* (CRC, Cleveland, 2003).
[23] J.-Y. Bigot, V. Halté, J.-C. Merle, and A. Daunois, Chem. Phys. **251**, 181 (2000).
[24] W. S. Fann, R. Storz, H. W. K. Tom, and J. Bokor, Phys. Rev. B **46**, 13592 (1992).
[25] M. Perner, P. Bost, U. Lemmer, G. von Plessen, J. Feldmann, U. Becker, M. Mennig, M. Schmitt, and H. Schmidt, Phys. Rev. Lett. **78**, 2192 (1997).
[26] N. Del Fatti, C. Voisin, M. Achermann, S. Tzortzakis, D. Christofilos, and F. Vallée, Phys. Rev. B **61**, 16956 (2000).
[27] S. I. Anisimov, B. L. Kapeliovich, and T. L. Perel'man, Sov. Phys. JETP **39**, 375 (1974).
[28] H. E. Elsayed-Ali, T. Juhasz, G. O. Smith, and W. E. Bron, Phys. Rev. B **43**, 4488 (1991).